PV architectures for DC microgrids using buck or boost exclusive microconverters

Marafante, E; Mackay, LJ; Hailu, TG; Chandra Mouli, GR; Ramirez Elizondo, LM; Bauer, P

DOI
10.1109/PTC.2015.7232733

Publication date
2015

Document Version
Accepted author manuscript

Published in
Proceedings of the 2015 IEEE Eindhoven PowerTech

PV Architectures for DC Microgrids using Buck or Boost Exclusive microconverters

Emanuele Marafante, Laurens Mackay, Tsegay Gebremedhin Hailu,
Gautham Ram Chandra Mouli, Laura Ramirez-Elizondo, Pavol Bauer
Delft University of Technology, the Netherlands
l.j.mackay@tudelft.nl

***Abstract*—DC microgrids can connect directly dc renewable energy sources with increasing amount of dc loads. In this paper it is looked for possible architectures for integrating PV panels into DC microgrids by means of microconverter strings. Three topologies are considered featuring only buck microconverters and only boost microconverters which promise higher efficiency due to fewer semiconductors in the current path.**

***Index Terms*—dc microgrid, microconverter, pv, pv string.**

I. Introduction

The latest gathered data [1] about the worldwide increase in renewable electricity generation have even shown how the previous-year predictions had been underestimated; electrical energy coming from sustainable sources has now reached the one produced via natural gas (22 %).

As of today, electrical photovoltaic power installed amounts to about 180 GWp [1], while projections make this quantity increase to 690 GWp in the next 20 years [2], with 50% capacity divided among China, UE and USA.

The goals to be reached by power electronics equipment in a currently-in-use PV system are basically two: the inversion (conversion from DC power to the AC power of the grid and household utilities), to one phase for low powers or to three phases for higher powers (3-5 kW or more), and the maximum power point tracking (MPPT) [3]. Other converters may deal with the voltage level adjustment, if needed. The need for a working power electronics equipment, alongside with the strain to reach a always-better system management, have ended in the development of different solutions for the connection of solar panels to the today-in-use AC grid. The system architectures commonly found in literature are four: central inverter (one inverter for all the panels), multi-string inverters (one single inverter receiving a DC bus where all the panels' strings are connected through DC/DC converters), string inverters (one low-power inverter for every modules' string) and module inverter or AC module [4]. More complex solutions come with higher initial cost. However, in the literature, articles are found which claim that the investment will be recovered due to a better performance [5]. This is due to the fact that connecting all the modules to the same MPPT system (usually embedded in the inverter) results in higher losses [3] because of the different illumination conditions, while shading and unavoidable mismatches force connected panels to work at their minima either of current or voltage, depending on their connection.

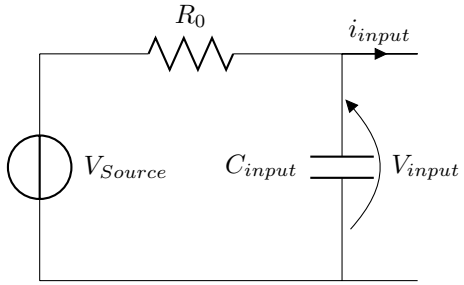

Fig. 1. Circuitry used to simplify a solar panel's power vs voltage curve

No example in the literature dealing with the connection of a PV array to a DC distribution grid other than the DC bus of the multi-string inverter architecture was found. DC-microgrids are, on the other hand, driving interests for their potential in losses reduction, while allowing the interconnection of DC-generating renewable sources (not only PV panels, but also fuel cells), electrical energy storage and loads (LEDs, computers, cellphones...). The energy saving is given by the missing inversion-rectification passages, currently happening in our households' electrical systems [6].

Different topologies have been proposed for a low-voltage DC (LVDC) grid; they are mainly monopolar or bipolar, with or without additional neutral wire [2]. Also the voltage level has to be set, keeping in mind that it will affect the Ohmic losses in the cables. The upper limit for the LVDC voltage has already been fixed to 1500 V by IEC 60364, although standardisation, being it of nominal voltage, voltage range and safety measures is developing [7].

In this paper, the optimal system architecture for a series-connected PV array, featuring modular DC/DC mircoconverters and a central converter to interface with a DC microgrid, will be investigated. Each modular microconverter will provide a dedicated maximum power point tracking; the central dc microgrid converter will take car of the grid connection.

II. Only buck or only boost more efficient

The study "Cascaded DC/DC converters connection of photovoltaic modules" [5] has analysed the issue of having a

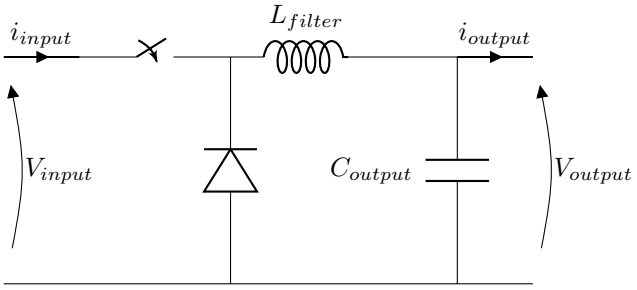

Fig. 2. Buck converter

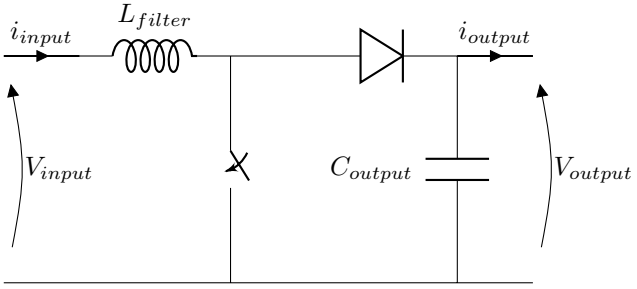

Fig. 3. Boost converter

series connection of panels with dedicated converters, focusing on the efficiency in the power transfer. From their simulations and experimental results it is seen how the best efficiency is obtained in case of buck dedicated converters 2, while boost converters 3 perform slightly worse; buck-boost and Cuk converters instead show a lagging performance. The losses become of course more important if the power rating of the system increases; the system, although versatile, shows an inferior power transfer performance.

For this reason in this paper it is especially looked at micro-converters that can only increase or only decrease the output voltage of the PV panel. Due to the fewer semiconductors in the current path they promise lower conduction losses and thus higher efficiency. microconverters will be operated without communication.

III. DC Microgrid Side Converter

A central dc/dc converter will connect single or muliple strings to the grid. A natural choice to couple a series of converters of a kind is the conjugated type: panel-dedicated buck microconverters will require a boost converter to interface with the LVDC grid, and vice versa. The first option allows the black start from low voltages and guarantees that the voltage in the DC link sticks to a reasonable value, while the second could not prevent current from flowing into a short circuited DC microgrid. However, to deal with a wider range of voltages and take advange of both, a solution using a non-inverting buck-boost topology as central converter will be taken into account. A more efficient central converter could reduce the voltage ratio of the microconverters and thus efficiency by adapting the string voltage and current.

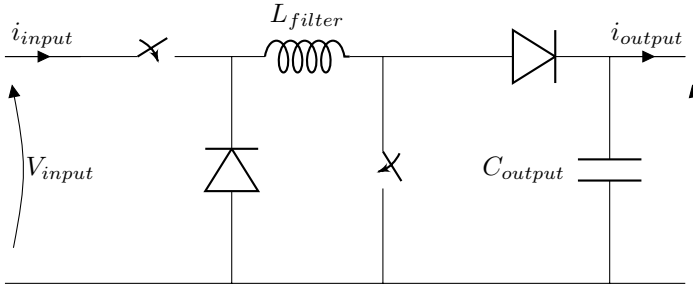

Fig. 4. Non-inverting buck-boost converter

P&O: Reference variation as function of previous power and reference variations	Δ power previous step > 0	Δ power previous step < 0
Δ reference previous step > 0	New Δ reference step > 0	New Δ reference step < 0
Δ reference previous step < 0	New Δ reference step < 0	New Δ reference step > 0

Fig. 5. Logic of perturb & Observe algorithm

IV. The control scheme used

The MPPT is performed through perturb & observe (P&O) algorithm. The basic logic underneath this scheme is represented in Fig. 5: as described in [8], this easily-implemented algorithm has the drawback of struggling with irradiance changes. This problem will be dealt with using the tracking capability of the treated dual-converter-layer scheme, and with a fast repetition of this control. The reference parameter, output of the P&O controller, is the input voltage for the microconverters. The central converter instead maintains the link current stable. For every converter, reference and actual values will be then combined and fed to a PI controller, which will convert them into the new duty cycle. While the control loop is continuous, the references are reset every 100 ms for the microconverters, and every 10 ms for the central converter.

V. Case Study

Three topologies are considered: modular buck converters and central boost converter (Fig. 6), modular buck and central boost (Fig. 10), modular buck and central non-inverting buck-boost (Figure 14), the last converter made by a buck converter in series with a boost one. The scope of this paper is testing the MPP tracking ability that single microconverters have, without communication through a P&O algorithm. The converters have been modeled in averaged mathematical form. This has involved modeling the electrical components with their governing equations, and allowed to speed up the simulations, while retaining useful insight in the converters' behavior. The number of microconverters in series has been chosen to be 10. The grid voltage is varied from case to case (see Fig. 6, 10 and 14) so that, with full irradiance, the microconverters can apply maximum power point at their maximum efficiency duty cycle (1 for buck and 0 for boost converters) [9]. Of course

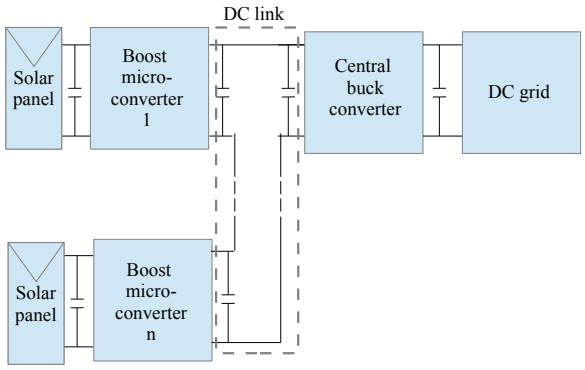

Fig. 6. Boost microconverters and buck central converter topology

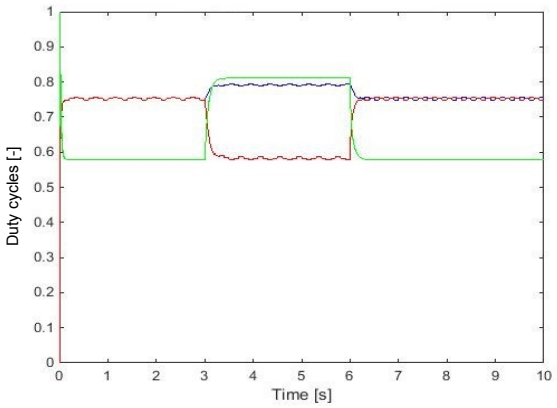

Fig. 7. Case 1: the duty cycles of the converters with full irradiance are in blue, while the other ones' are in red. The duty cycle of the central converter is depicted in green.

the grid could have been considered of the same voltage every time, but this would increase the number of microconverters in the boost case, thus slowing down the simulations without increasing their insight. Shading is simulated by increasing the source resistance (see Fig. 1) for some time. The total power at full irradiance is 600 W, with each source module giving 60 W sporting a voltage source V_{source}=30 V and a resistor R_0=3.75 Ω.

A. Case 1: Boost microconverters with Buck DC grid converter

The voltage of the microgrid for this case is fixed to 100 V. The system's voltage, in steady state, follows the equation

$$V_{\text{grid}} = \eta_{\text{Buck,v}}\delta_{\text{Buck}}V_{\text{link}} = \eta_{\text{Buck,v}}\delta_{\text{Buck}}\sum_{i=1}^{n}\frac{\eta_{\text{Boost,v,i}}V_{\text{panel,i}}}{1-\delta_{\text{Boost,i}}} \quad (1)$$

Where V are the voltages, η the efficiencies of conversion and δ the duty cycles of the converters. The schematic is reproduced in Fig. 6. Considering that the panels are connected in series, and that the generated current is approximately proportional to the irradiance G, the following expression has to be satisfied for converters i and j in MPP in steady state:

$$I_{\text{link}} = I_{\text{panel},i}(1-D_i) = I_{\text{panel},j}(1-D_j) \quad (2)$$

and so

$$G_{\text{panel},i}(1-D_i) = G_{\text{panel},j}(1-D_j) \quad (3)$$

and

$$D_i = 1-(1-D_j)\frac{G_{\text{panel},j}}{G_{\text{panel},i}} \quad (4)$$

It follows from this equation that, if $G_j < G_i$, the microconverter of panel i cannot have duty cycle zero unless microconverter j has an absurd negative duty cycle. Analogously, if $D_j = 0, D_i$ can only be a strictly positive number. Fig. 7, 8

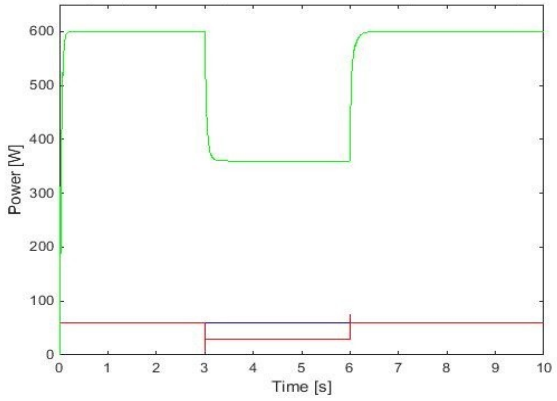

Fig. 8. Case 1: in blue the power produced by a single module in the unshaded case, in red the one with shading, in green the total power from the modules.

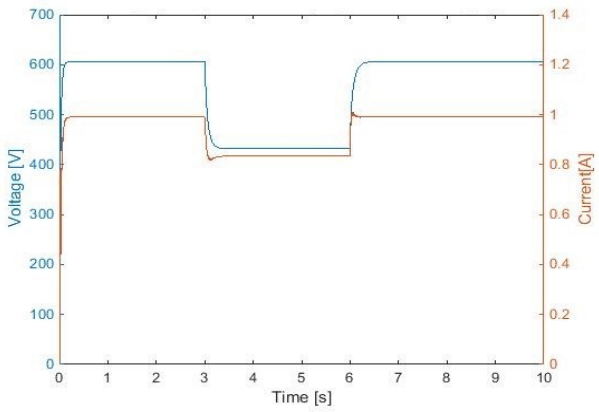

Fig. 9. Case 1: the voltage in the DC link is depicted in blue, the current is in red.

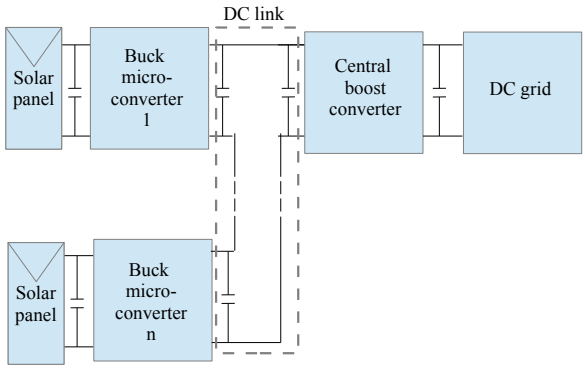

Fig. 10. Buck microconverters and boost central converter topology

and 9 show the results of the shading experiment of Case 1. In the period between 3 s and 6 s, of the 10 s of simulation, the source resistances of modules 3 to 10 are doubled, thus mimicking an halving in the irradiance: the power available is reduced to 360 W. It can be seen how the duty cycles of the full-irradiance panels have to increase in case of shading. This system is quite far from the duty cycle values that allow the best efficiency; it also reacts slowly with respect to the other topologies.

B. Case 2: Buck microconverters with Boost DC grid converter

The schematic is depicted in Fig. 10. The equation for the voltage is, in this case,

$$V_{\text{grid}} = \frac{\eta_{\text{Boost,v}} V_{\text{link}}}{1-\delta_{\text{Boost}}} = \frac{\eta_{\text{Boost,v}} \sum_{i=1}^{n} \eta_{\text{Buck,v,i}} V_{\text{panel,i}} \delta_{\text{Buck,i}}}{1-\delta_{\text{Boost}}} \quad (5)$$

The grid voltage is fixed to 350 V. Using the same line of reasoning as for Case 1, the following equations can be written:

$$\frac{G_{\text{panel, } j}}{\delta_j} = \frac{G_{\text{panel},j}}{\delta_j} \quad (6)$$

$$\delta_i = \delta_j \frac{G_{\text{panel},i}}{G_{\text{panel},j}} \quad (7)$$

Therefore, this time the converters connected to a shaded source will have to move from the most efficient configuration, decreasing their duty cycles. Fig. 11, 12 and 13 show the same experiment tried for Case 1. It can be seen how the current is almost maintained in the link, while the duty cycles of the lower-yielding converters decrease. This schematic operates in the range of the highest efficiencies for the microconverters.

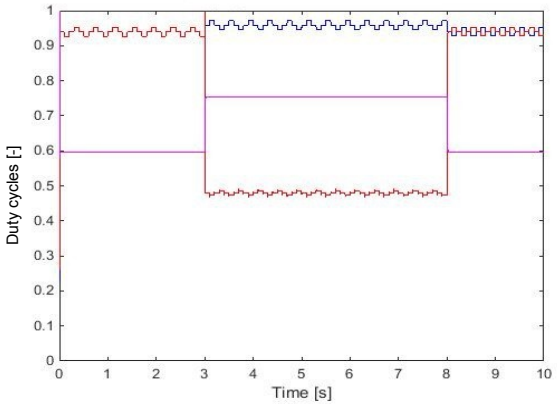

Fig. 11. Case 2: the duty cycles of the converters with full irradiance are in blue, while the other ones' are in red. The duty cycle of the central converter is depicted in purple.

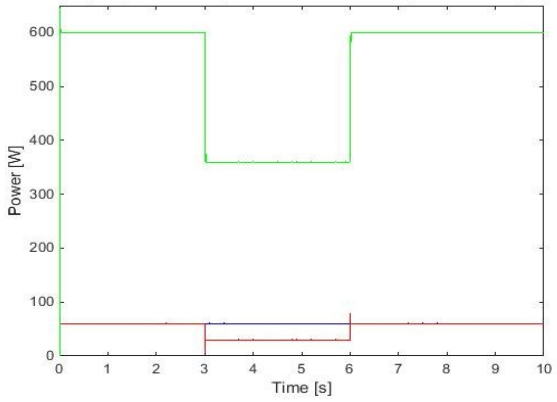

Fig. 12. Case 2: in blue the power produced by a single module in the unshaded case, in red the one with shading, in green the total power from the modules.

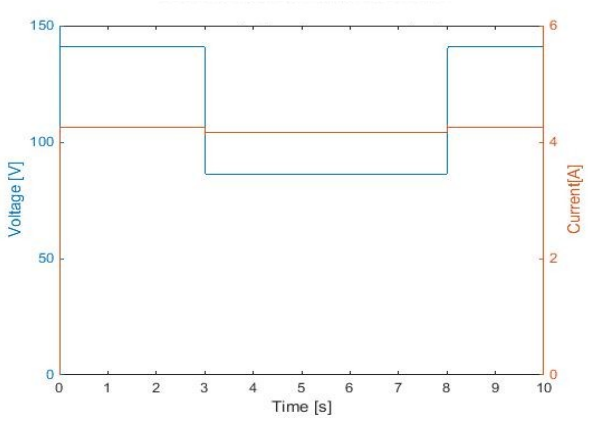

Fig. 13. Case 2: the voltage in the DC link is depicted in blue, the current is in red.

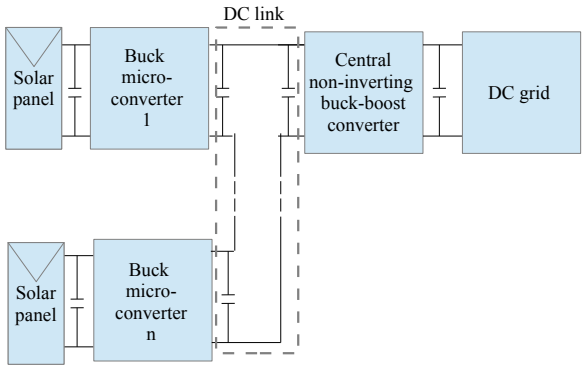

Fig. 14. Buck microconverters and non-inverting buck-boost central converter topology

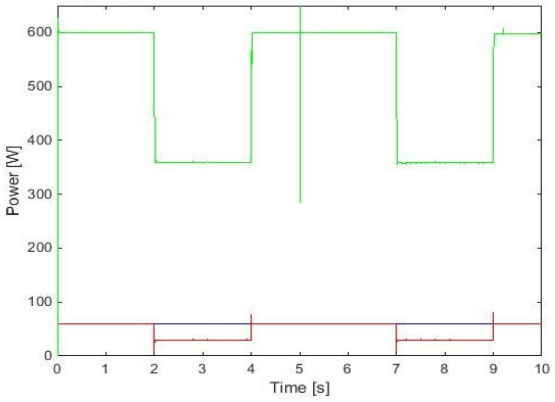

Fig. 16. Case 3: in blue the power produced by a single module in the unshaded case, in red the one with shading, in green the total power from the modules.

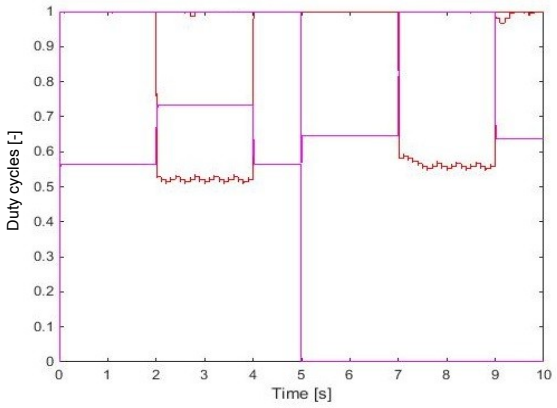

Fig. 15. Case 3: the duty cycles of the unshaded modules are almost invisible because they stick to 1; the shaded ones are in red. The buck-boost's duty cycles are in purple.

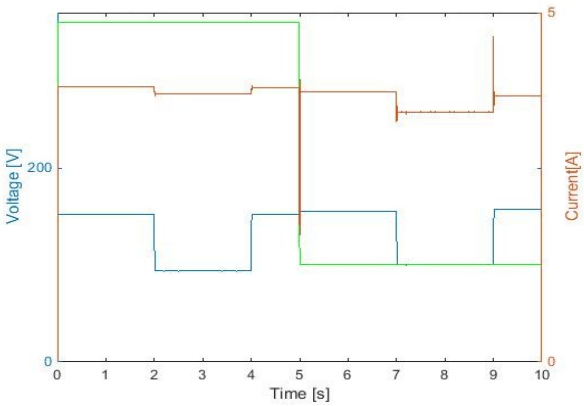

Fig. 17. Case 3: the voltage in the DC link is depicted in blue, the current is in red; the voltage in the connected microgrid is depicted in green.

C. Case 3: Buck microconverter with Buck-Boost DC grid converter

The regulating equation is, this time,

$$V_{\text{grid}} = \frac{\eta_{\text{Buck-Boost,v}}\delta_{\text{Buck-Boost,1}}}{1-\delta_{\text{Buck-Boost,2}}}V_{\text{link}} = \eta_{\text{Buck-Boost,v}}\frac{\delta_{\text{Buck-Boost,1}}}{1-\delta_{\text{Buck-Boost,2}}}\sum_{i=1}^{10}\eta_{\text{Buck,v,i}}V_{\text{panel,i}}\delta_{\text{Buck,i}} \tag{8}$$

This scheme's best operation is achieved when the tracking can be performed by the central converter only, while all the modules share the same irradiance and duty cycle 1. This is possible, with a continuous control scheme, if the P&O algorithm manages to take to 1 the duty cycles of the microconverters before the central converter has stabilized. With this sentence, we mean either duty cycle 1 (buck part of the buck-boost) or 0 (boost part). This time, both the modes are tested in a single experiment: first, the grid voltage is fixed to 350 V for 5 s, with shading as for Case 1 and 2 from 2 s to 4 s; then, in the following 5 s the grid voltage is 100 V and the shading is applied in the period 7-9 s. In Fig. 15 it can be seen that the most efficient configuration is actually respected, while Fig. 16 and 17 report the behavior of the system. The buck-boost commands only one of its switches at a time; the abrupt transition causes overshoot, but with constant output voltage the operation is stable. Two different PI controllers are needed for the buck and boost parts.

VI. Different irradiances test

Another experiment has been performed to check the ability of MPPT for different irradiances all over an array. Source resistors of different sizes (R_0, $2R_0$, $3R_0$, $4R_0$, $5R_0$ and open circuit) have been used for 5 s; Case 3 has 2.5 s at 350 V load ans 2.5 s at 100 V load. A case of complete shading has been added. The results are depicted in Fig. 18,

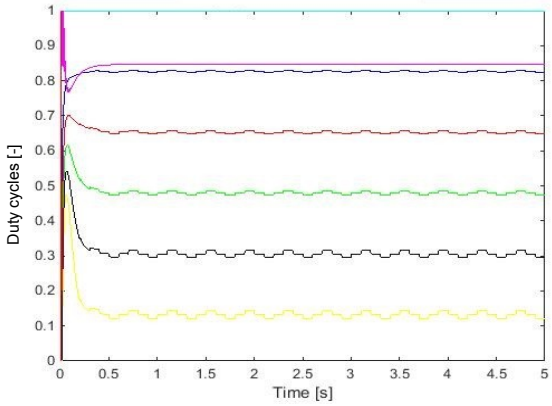

Fig. 18. Case 1: duty cycle disposition due to different irradiances

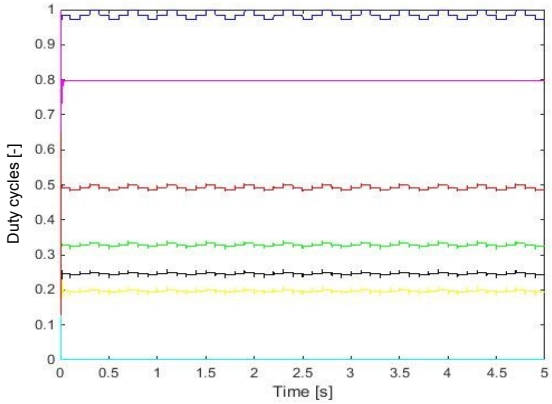

Fig. 19. Case 2: duty cycle disposition due to different irradiances

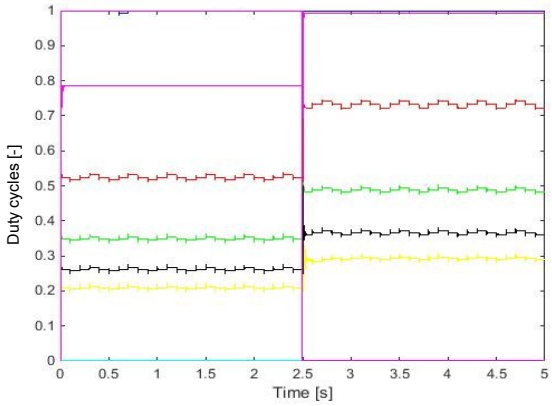

Fig. 20. Case 3: duty cycle disposition due to different irradiances

19 and 20. It can be seen how the duty cycles dispose based on the irradiance, as per equations 4 and 7; the converter with no irradiance (open-circuited source) is cut out in all the cases. This is done by giving duty cycle 0 to the buck microconverters (cyan line in Fig. 19 and Fig. 20) or 1 to the boost microconverters (cyan line in Fig. 18) Again, the configuration with boost microconverter lags in response time, while the other topologies offer a better performance (buck microconverter) and versatility (boost microconverter).

VII. Conclusion

The performance of a DC-link controller with microconverters and a central converter are analysed; three topologies are considered. The resulting response to the inputs is shown to be satisfactory, and the topologies described in Cases 2 and 3 have shown a better behavior with respect to the topology of Case 1. Further research is expected in order to optimize the control scheme of the converters, so that they always operate with their best efficiency.

References

[1] IEA (International Energy Agency), "Renewable energy medium term market report 2014 Market analysis and forecast to 2020," 2014.

[2] J. J. Justo, F. Mwasilu, J. Lee, and J.-W. Jung, "AC-microgrids versus DC-microgrids with distributed energy resources: A review," *Renewable and Sustainable Energy Reviews*, vol. 24, pp. 387–405, Aug. 2013. [Online]. Available: http://linkinghub.elsevier.com/retrieve/pii/S1364032113002268

[3] F. Blaabjerg, Z. Chen, and S. B. Kjaer, "Power electronics as efficient interface in dispersed power generation systems," *IEEE Transactions on Power Electronics*, vol. 19, pp. 1184–1194, 2004.

[4] K. Sun, L. Zhang, Y. Xing, and J. M. Guerrero, "A distributed control strategy based on DC bus signaling for modular photovoltaic generation systems with battery energy storage," *Power Electronics, IEEE ...*, vol. 26, no. 99, pp. 1–1, 2011. [Online]. Available: http://ieeexplore.ieee.org/xpls/abs_all.jsp?arnumber=5730500

[5] G. Walker and P. Sernia, "Cascaded DCDC Converter Connection of Photovoltaic Modules," *IEEE Transactions on Power Electronics*, vol. 19, no. 4, pp. 1130–1139, Jul. 2004. [Online]. Available: http://ieeexplore.ieee.org/lpdocs/epic03/wrapper.htm?arnumber=1310401

[6] L. Mackay, T. G. Hailu, G. R. Chandra Mouli, L. Ramirez-Elizondo, J. A. Ferreira, and P. Bauer, "From DC Nano- and Microgrids Towards the Universal DC Distribution System A Plea to Think Further Into the Future," in *PES General Meeting*. IEEE, 2015.

[7] M. Noritake, T. Iino, A. Fukui, K. Hirose, and M. Yamasaki, "A study of the safety of the DC 400 V distribution system," in *INTELEC, International Telecommunications Energy Conference (Proceedings)*, 2009.

[8] M. Rosu-Hamzescu and S. Oprea, "Practical Guide to Implementing Solar Panel MPPT Algorithms," 2013.

[9] N. Mohan and T. Undeland, *Power Electronics: Converters, Applications and Design*. Wiley, 2007.